



University
of Victoria



McGill

RUHR-UNIVERSITÄT BOCHUM
Institute of Geology, Mineralogy and Geophysics

Exploring possible causative mechanisms for earthquakes triggered by hydraulic fracturing: examples from the Montney Formation, BC, Canada

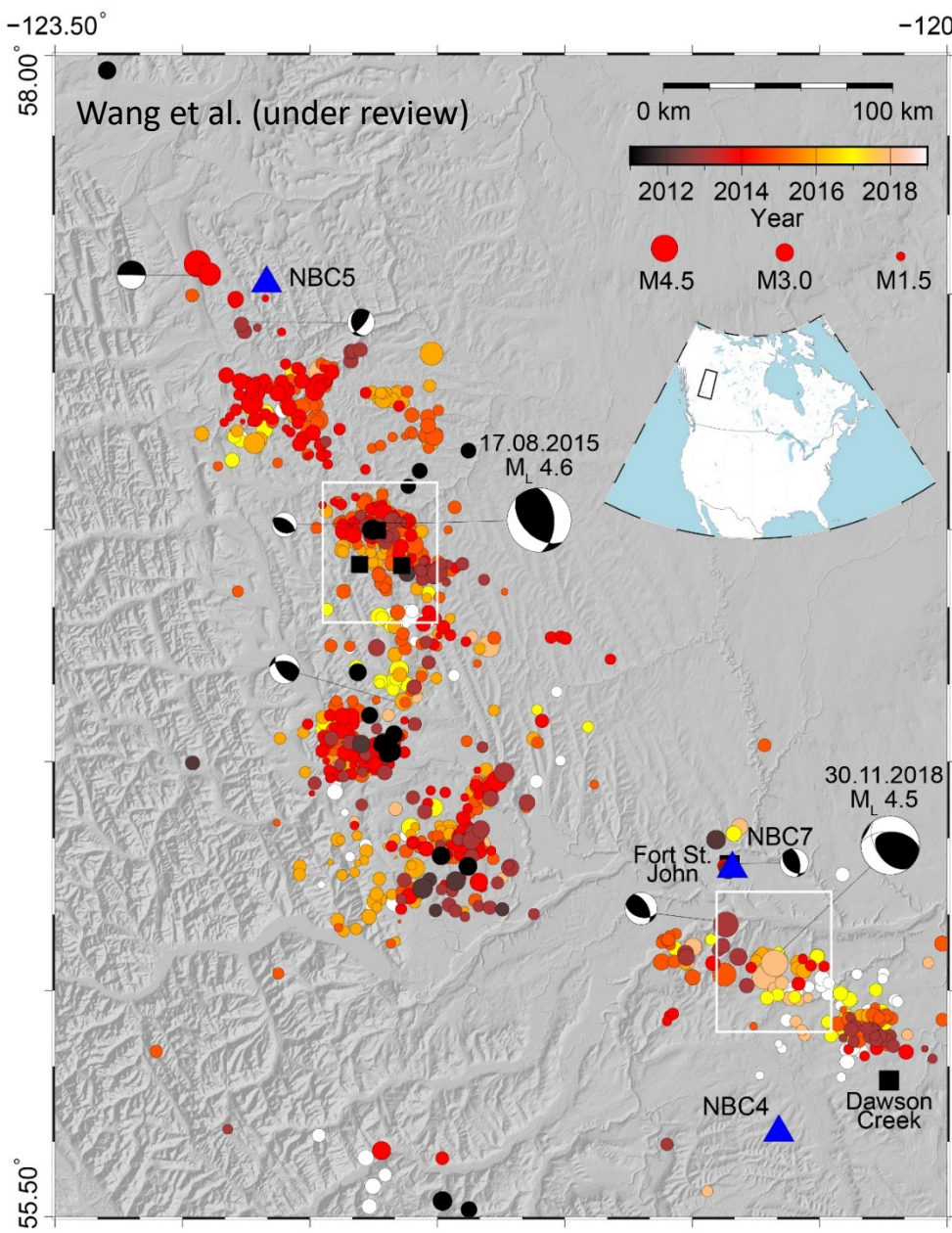
Alessandro Verdecchia¹, Bei Wang², Yajing Liu¹, Rebecca Harrington³, Marco Roth³,
Andres F. Peña Castro¹, and John Onwuemeka¹

¹McGill University, Montreal, Canada

²University of Victoria (UVic), Victoria, BC, Canada

³Ruhr-Universität Bochum, Germany

alessandro.verdecchia@mail.mcgill.ca



Seismicity in northeastern British Columbia for the period from 2011-2018. NRCAN stations in operation since 2011 shown in large triangles. Seismicity and focal mechanism solutions are from the NRCAN database.

We investigate the causative mechanisms for two large events in the Montney basin, British Columbia, the 17 August 2015 M_L 4.6 earthquake north of Fort St. John, and the 30 November 2018 M_L 4.5 earthquake which occurred near Dawson Creek. Both events are thought to have occurred within the crystalline basement, 1 to 2 km below the injected shale units (Montney formation).

Methods

Linear poroelasticity (Biot, 1941) to simulate pore pressure/elastic stress coupling (Comsol Multiphysics) in a 3D multilayered model. Pore pressure (Δp) and Coulomb stress changes calculations (ΔCFS).

The initial model includes **horizontal layers with different elastic and hydrological properties**. Two orders of magnitude lower permeability is assumed around the injected region to simulate permeability enhancement due to fracture opening.

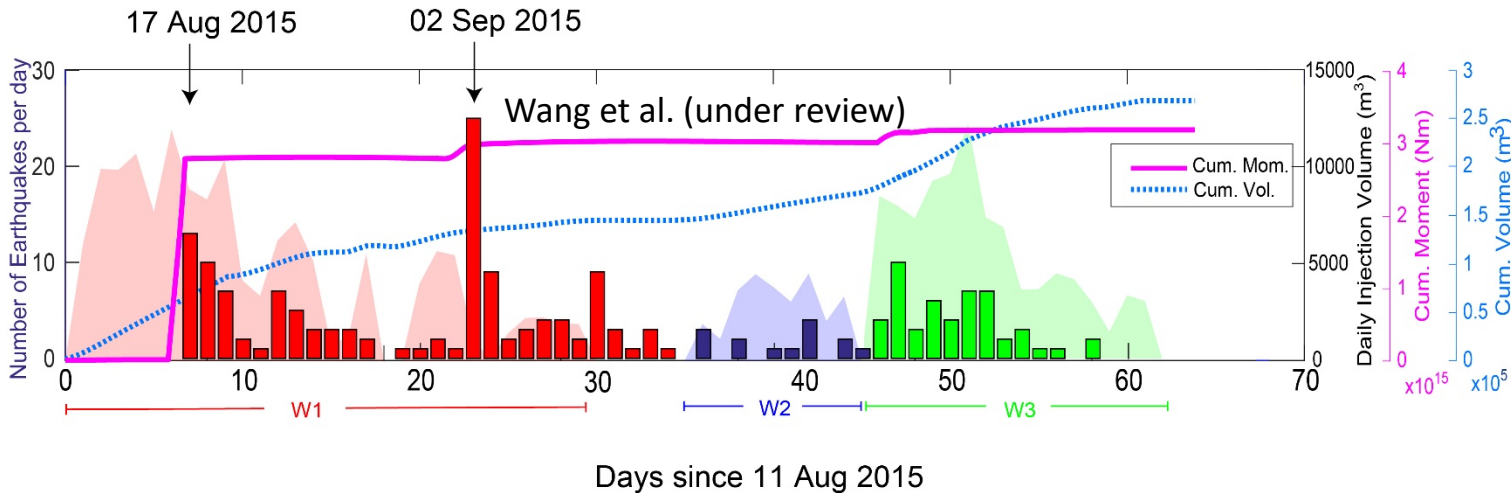
We built a second model which includes permeability anisotropies with an assumed permeability of $k=10^{-12}$ - 10^{-13} m² to simulate **high-permeability fluid conduits**.

Earthquakes detected using a **multi-station matched-filter (MMF)** method (Chamberlain et al., 2018, Peña Catro & Roth et al., in revision)

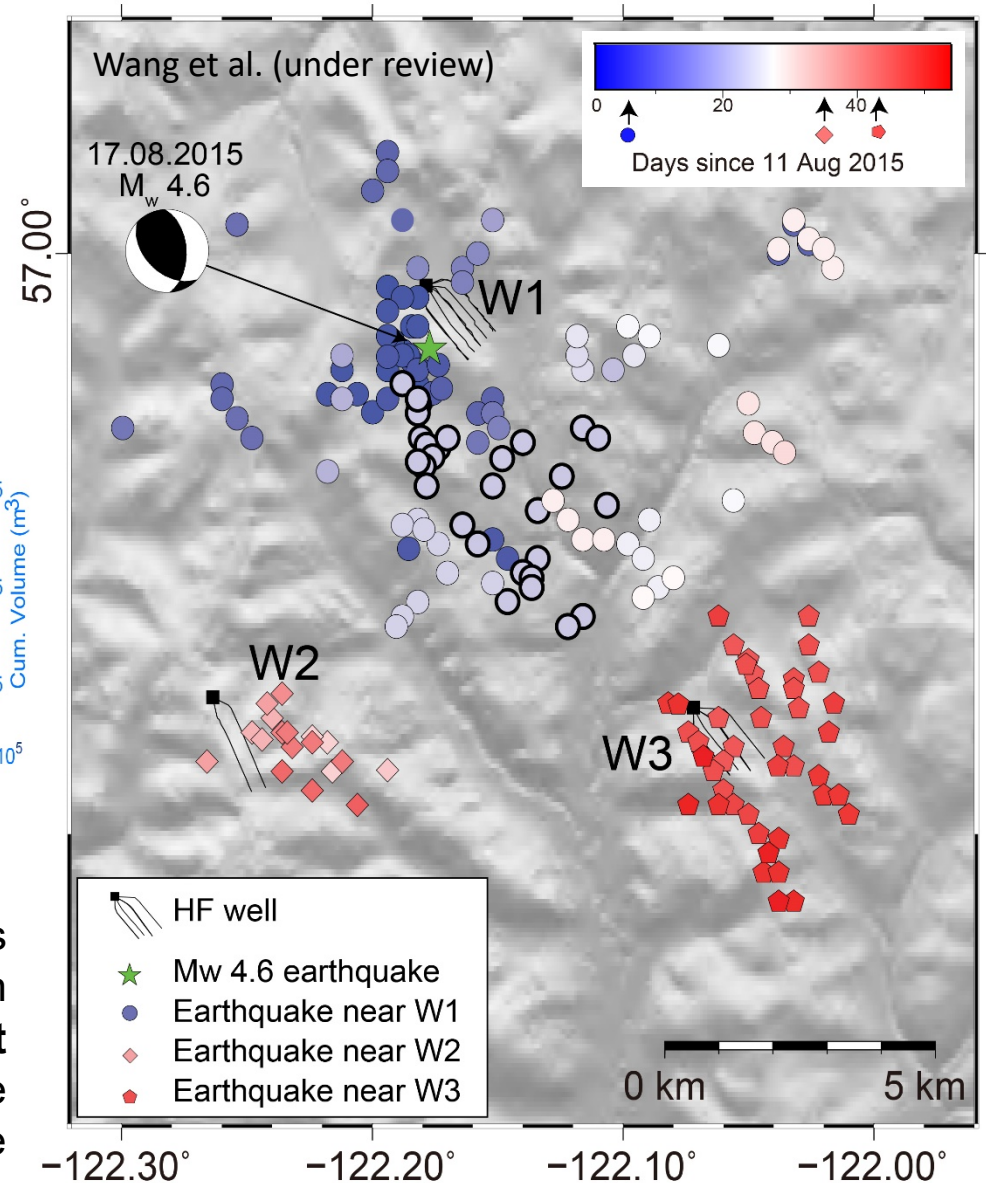
Earthquakes relocated using **HypoDD** (Waldhauser & Ellsworth, 2000).

The August 2015 sequence

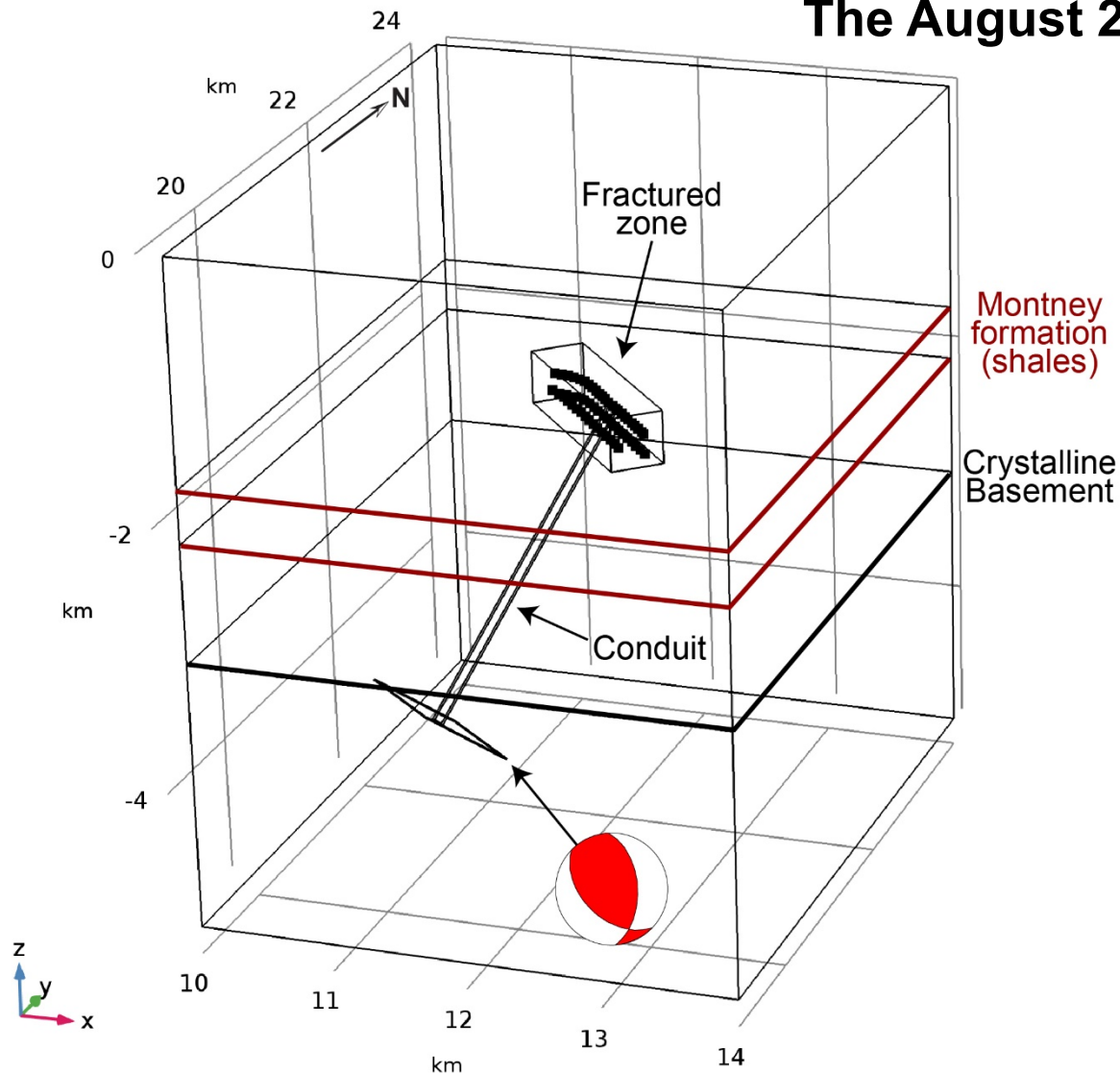
Relative relocations of 191 earthquakes detected using MMF detection. Horizontal well injection data is from the British Columbia Oil and Gas Commission (BCOGC) database. The star indicates the location of the **M_L 4.6 mainshock**. Symbol shapes differentiate clusters associated with respective hydraulic fracturing wells, W1, W2, and W3. Circles with thicker outlines denote earthquakes that occurred on 02 September 2015, the highest single-day seismicity rate.



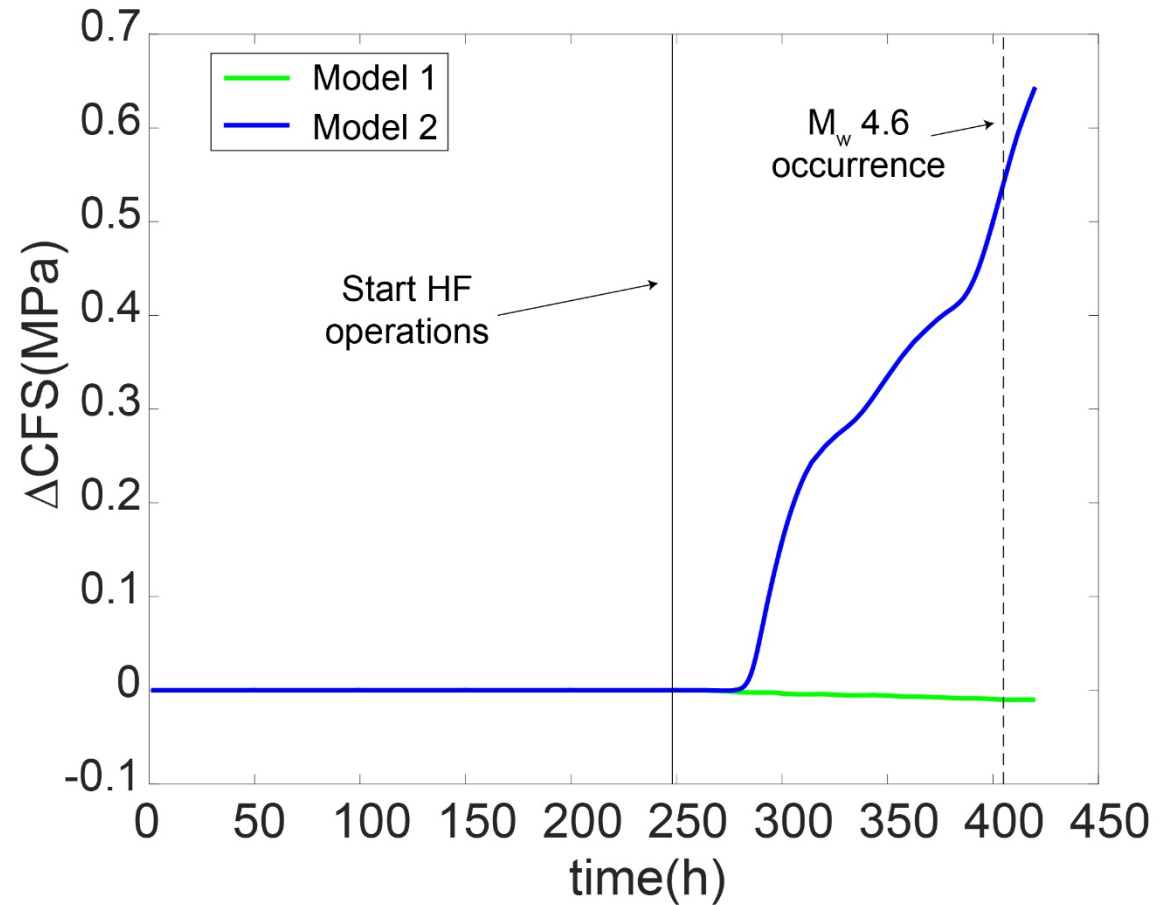
Daily seismicity versus daily injection volume. Daily injection data is indicated with the shaded areas, where bottom bars denote the injection activity for the different HF wells. Solid line indicates the **cumulative moment** for the MMF detected earthquakes shown in the histogram; dashed line denotes the **cumulative injection volume** from the three HF wells. The time starts from 11 August 2015, one day before the start of HF injection at W1.



The August 2015 sequence

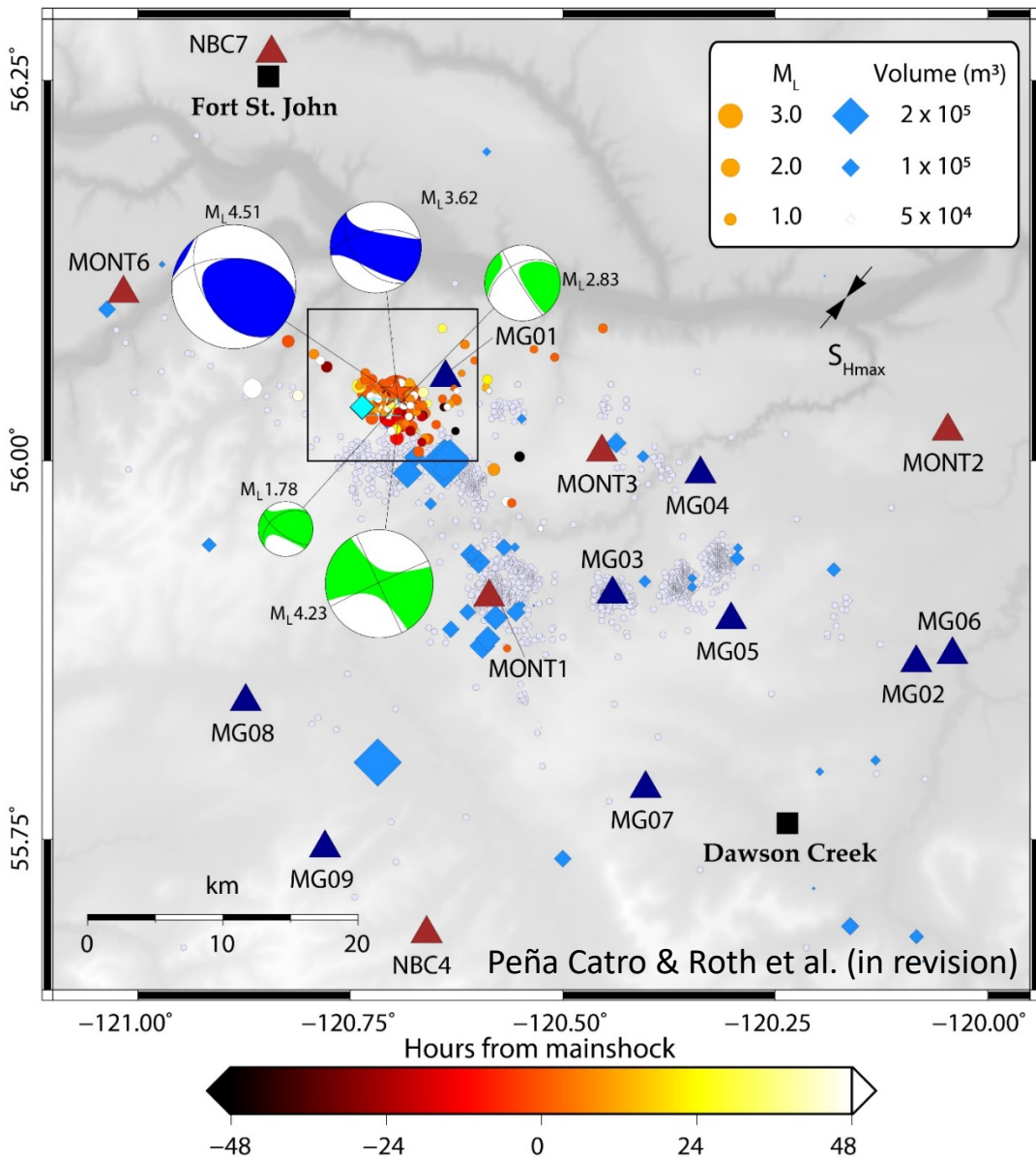


3D finite element model for the August 17 2015 M_L 4.6 earthquake. The model includes a region around the injection points with permeability values one order of magnitude larger than the shale formation, and a **conduit** connecting the injection zone modeled using a permeability contrast of 2-3 orders of magnitude.

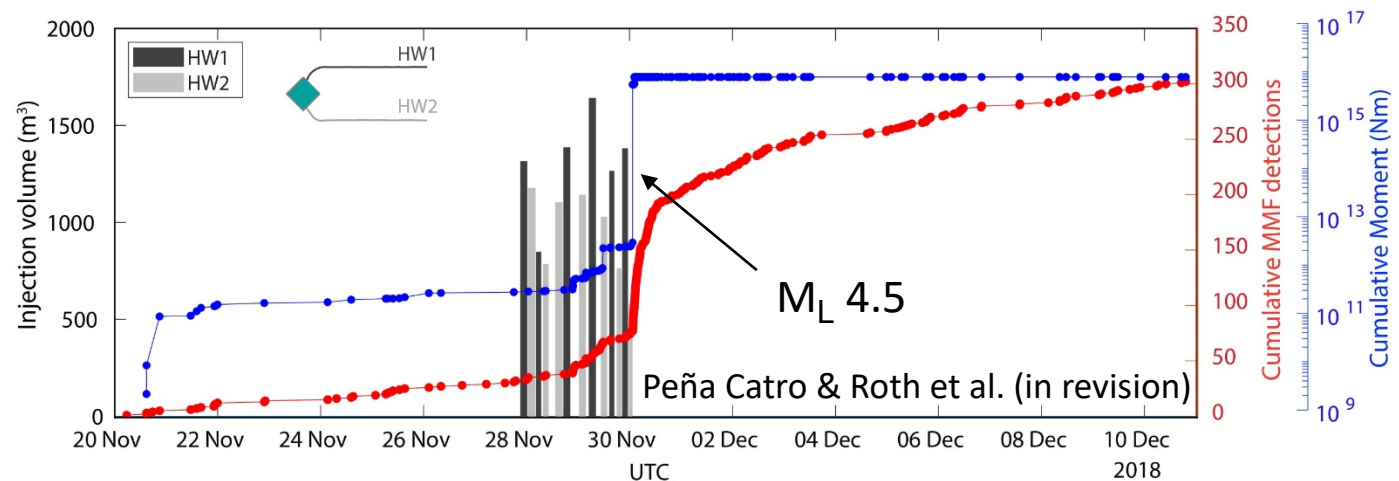


Coulomb stress changes evolution (ΔCFS) due to HF operations calculated on the location, geometry, and kinematics (strike 131° , dip 37° , rake 42°) of the M_L 4.6 earthquake. Model 1 does not include the conduit. Model 2 includes a conduit with permeability $k = 10^{-12} \text{ m}^2$.

The November/December 2018 sequence



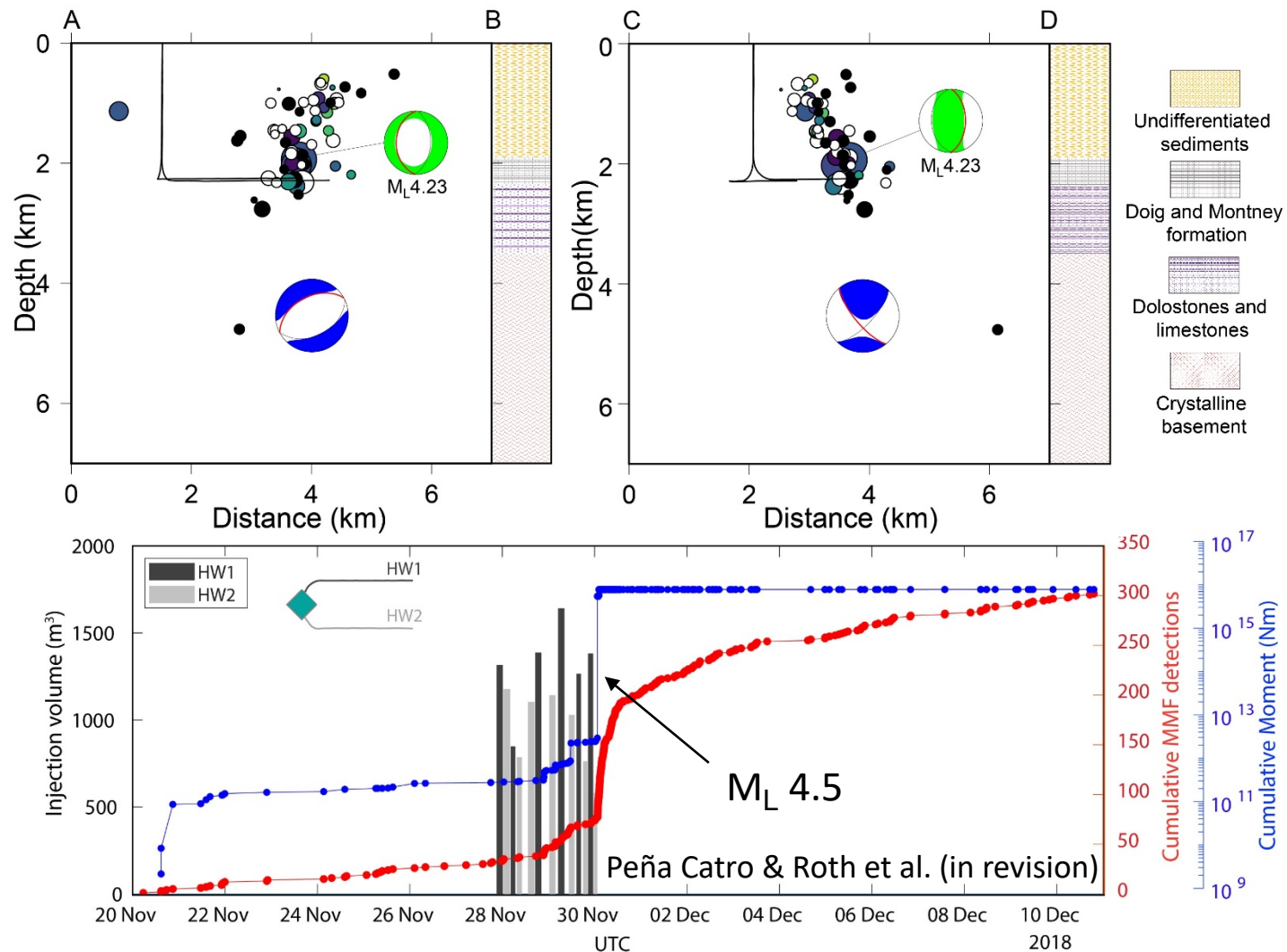
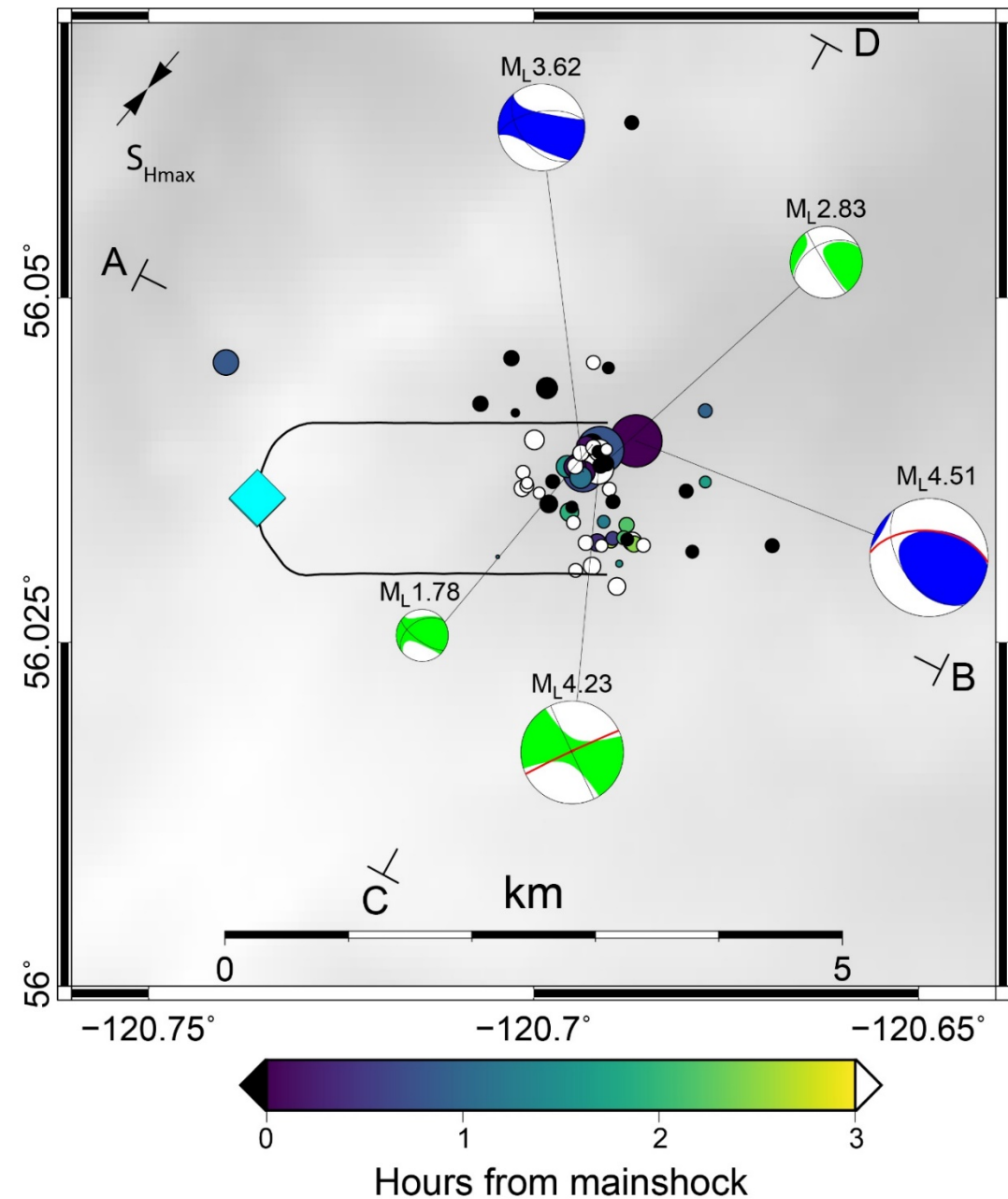
Earthquakes, seismic station, and hydraulic fracturing well distributions in the Dawson-Septimus area, northeast BC. Colored circles are MMF detected and located events 48 hours before and after the M_L 4.5 mainshock. MMF detections outside this period are colored in black (before) and white (after). Grey dots are **STA/LTA** detections January to December 2018. Blue diamonds are **active HF wells** in 2018 scaled by **injection volume**. Cyan diamond shows the well pad from which injection along two horizontal wells immediately preceded the M_L 4.5 event. S_{Hmax} represents regional maximum horizontal stress.



MMF-detected seismicity (red) and injection volume per stage (gray and black bars) along the two horizontal wells stimulated before the occurrence of the M_L 4.5. No other wells were stimulated within 15 km of the epicenter during this period. **Cumulative seismic moment** shown in blue.

The November/December 2018 sequence

Peña Catro & Roth et al. (in revision)

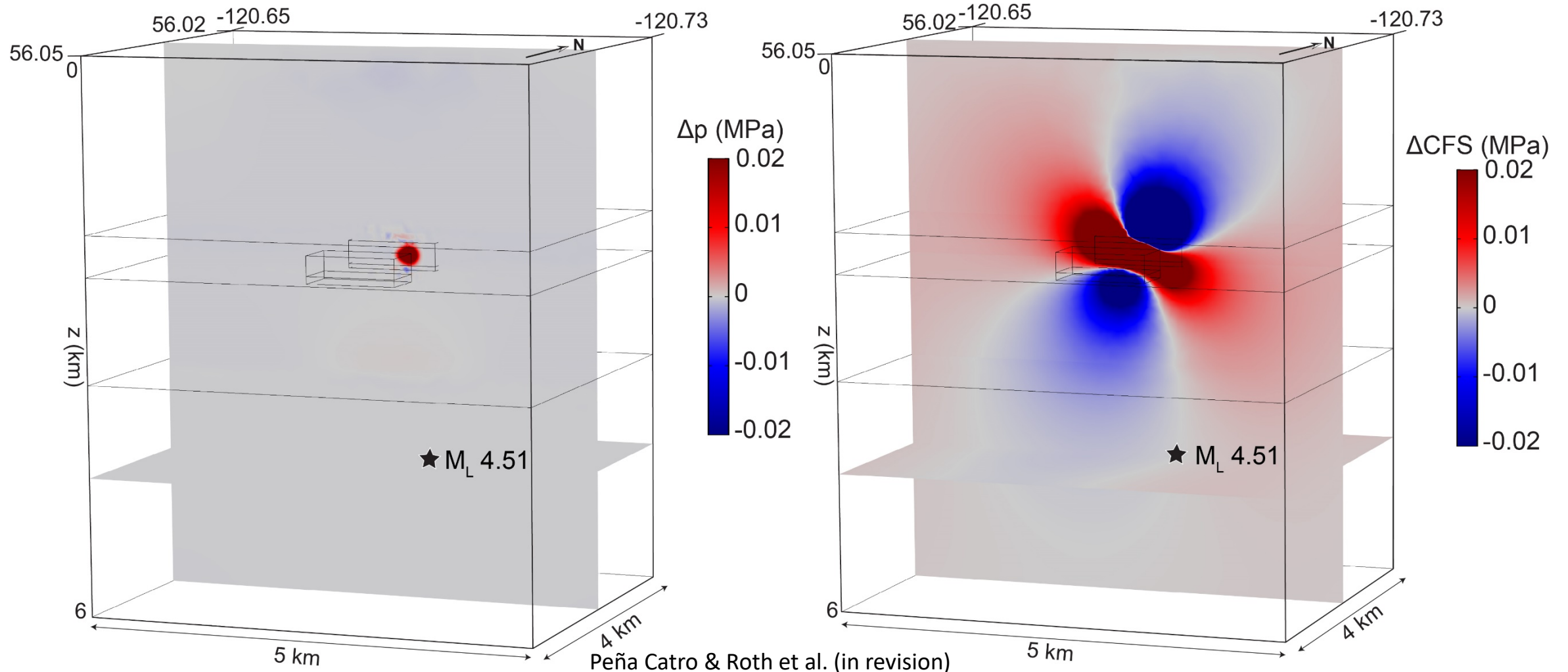


MMF-detected seismicity (red) and injection volume per stage (gray and black bars) along the two **horizontal wells stimulated** before the occurrence of the **M_L 4.5**. No other wells were stimulated within 15 km of the epicenter during this period. **Cumulative seismic moment** shown in blue.

The November/December 2018 sequence

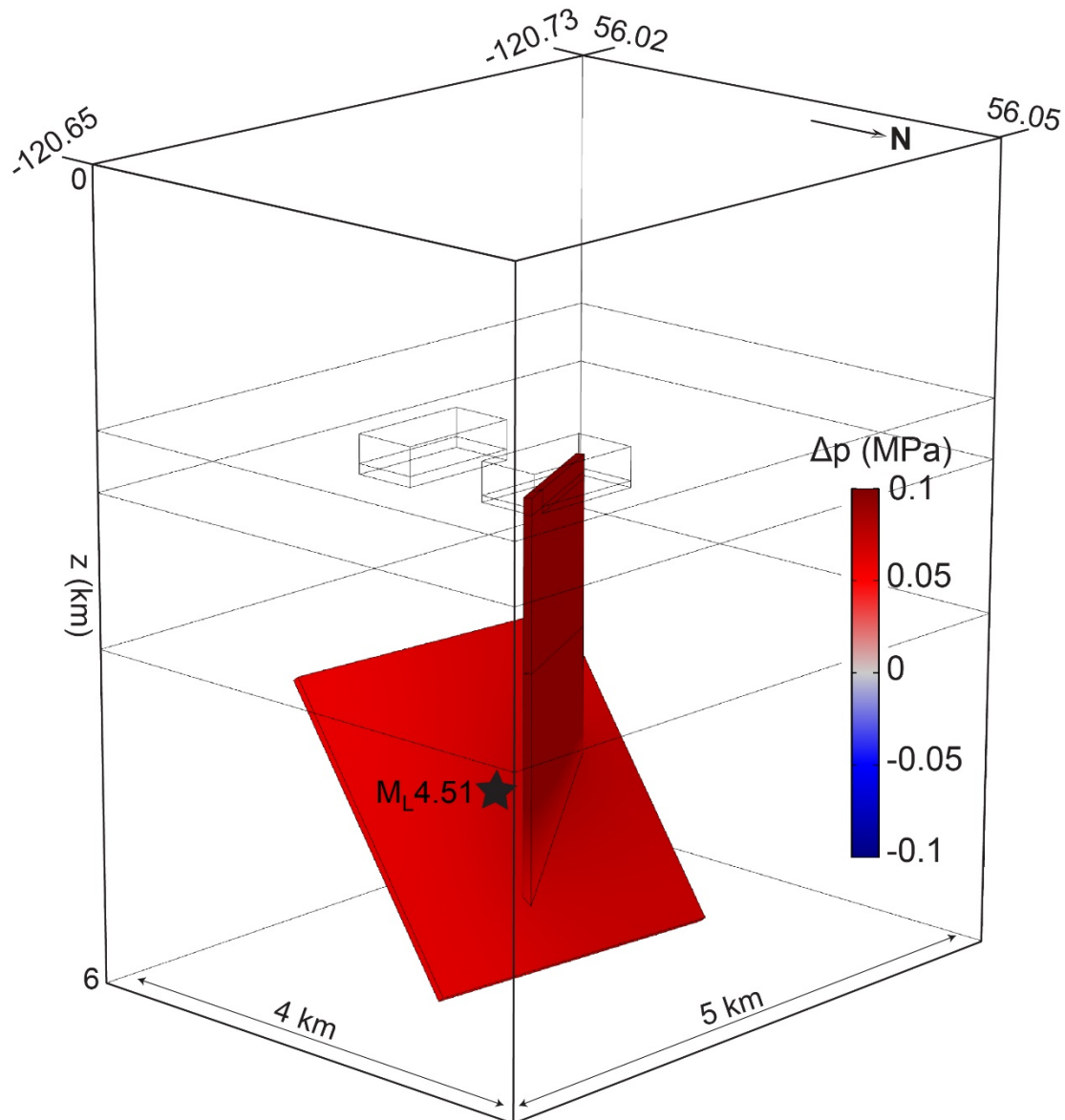
Poroelastic modeling

Pore pressure changes (Δp) (left) and Coulomb stress changes (ΔCFS) (right) due to fluid injection calculated based on the geometry and kinematics of the M_L 4.5 mainshock just before the occurrence of the earthquake using a poroelastic model without high-permeability fault zones. At the mainshock location we calculate no discernable pore pressure changes (left), and ΔCFS of 0.00015 MPa (right). These values are too small to explain triggering.



The November/December 2018 sequence

Poroelastic modeling and the conduit hypothesis



Pore pressure change Δp due to injection history along HW1 and HW2. Here, we introduce two **highly-permeable faults**. Permeability of $k= 10^{-12} \text{ m}^2$ is assumed along both the mainshock fault plane and a **vertical conduit** connecting the injection points to the mainshock fault. $k= 10^{-16}-10^{-19} \text{ m}^2$ elsewhere in the model domain

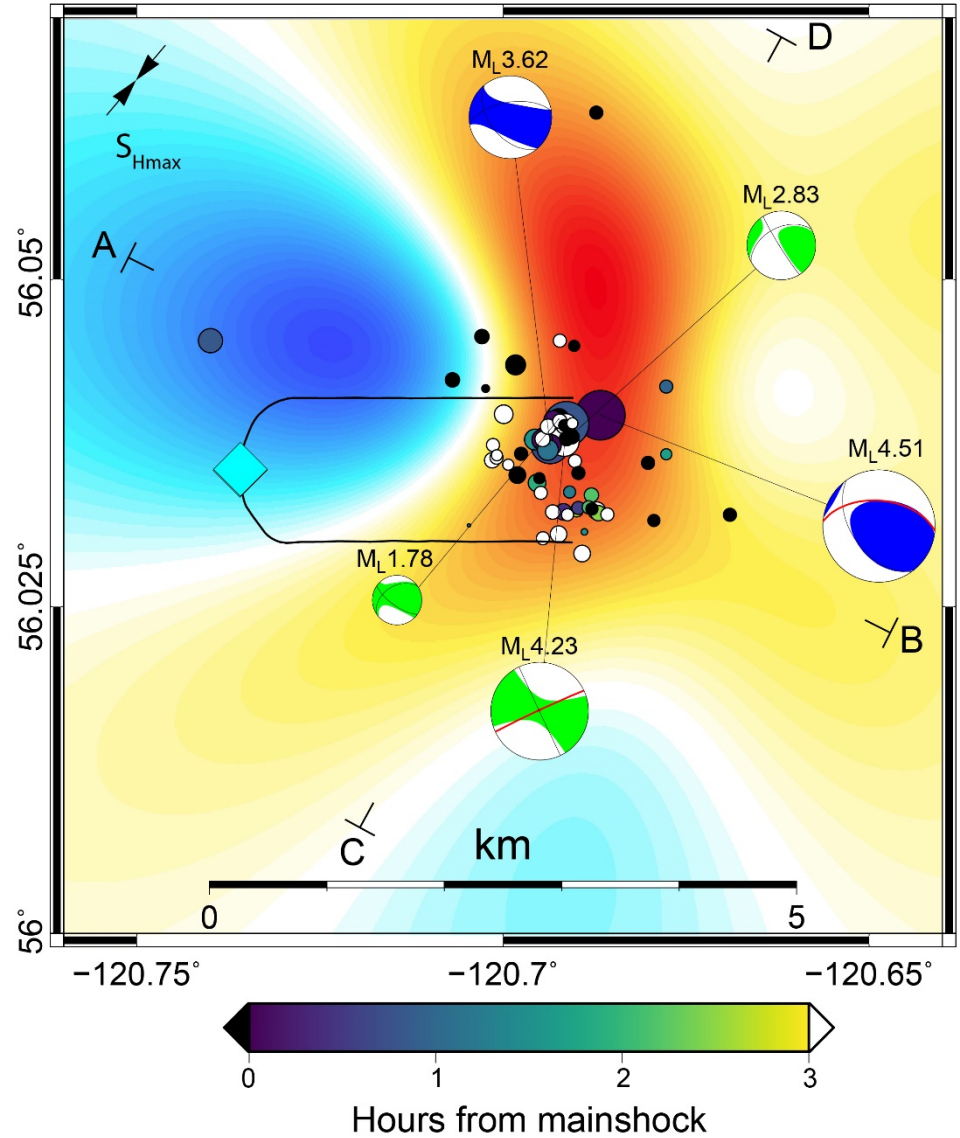
An **high-permeability conduit** is necessary to explain triggering of a mainshock located in the basement ($\sim 4.5 \text{ km}$ depth)

The **depth of the mainshock** is confirmed also by relocations done using **GrowClust** (Trugman & Shearer, 2017)

Canadian Natural Resources Limited (CNRL) placed the mainshock at **1.1 km depth** (Mahani et al., 2019, SRL). However, **no geodetically-observed coseismic ground deformation** has been detected in the region

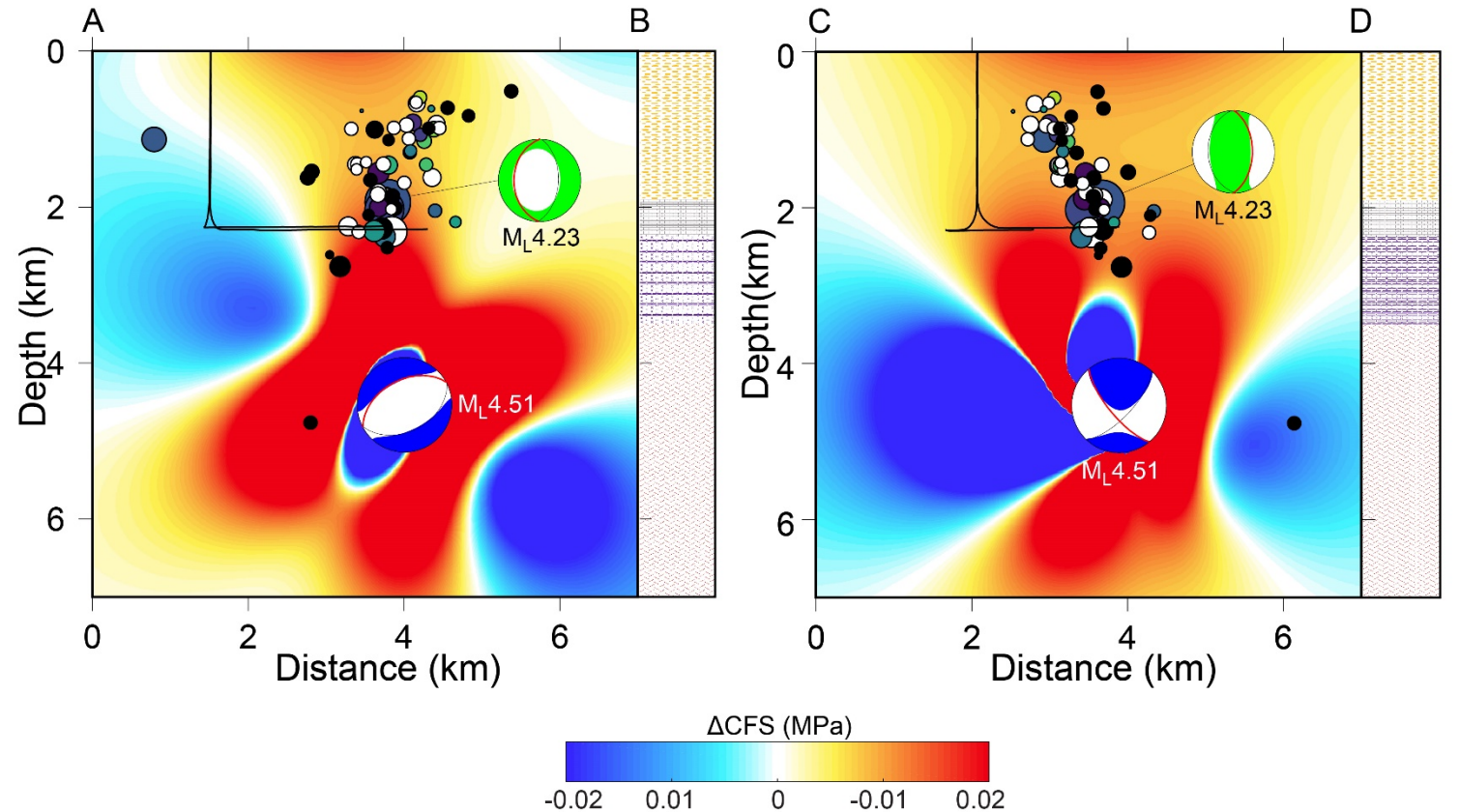
The November/December 2018 sequence

Coseismic Δ CFS vs. aftershocks distribution

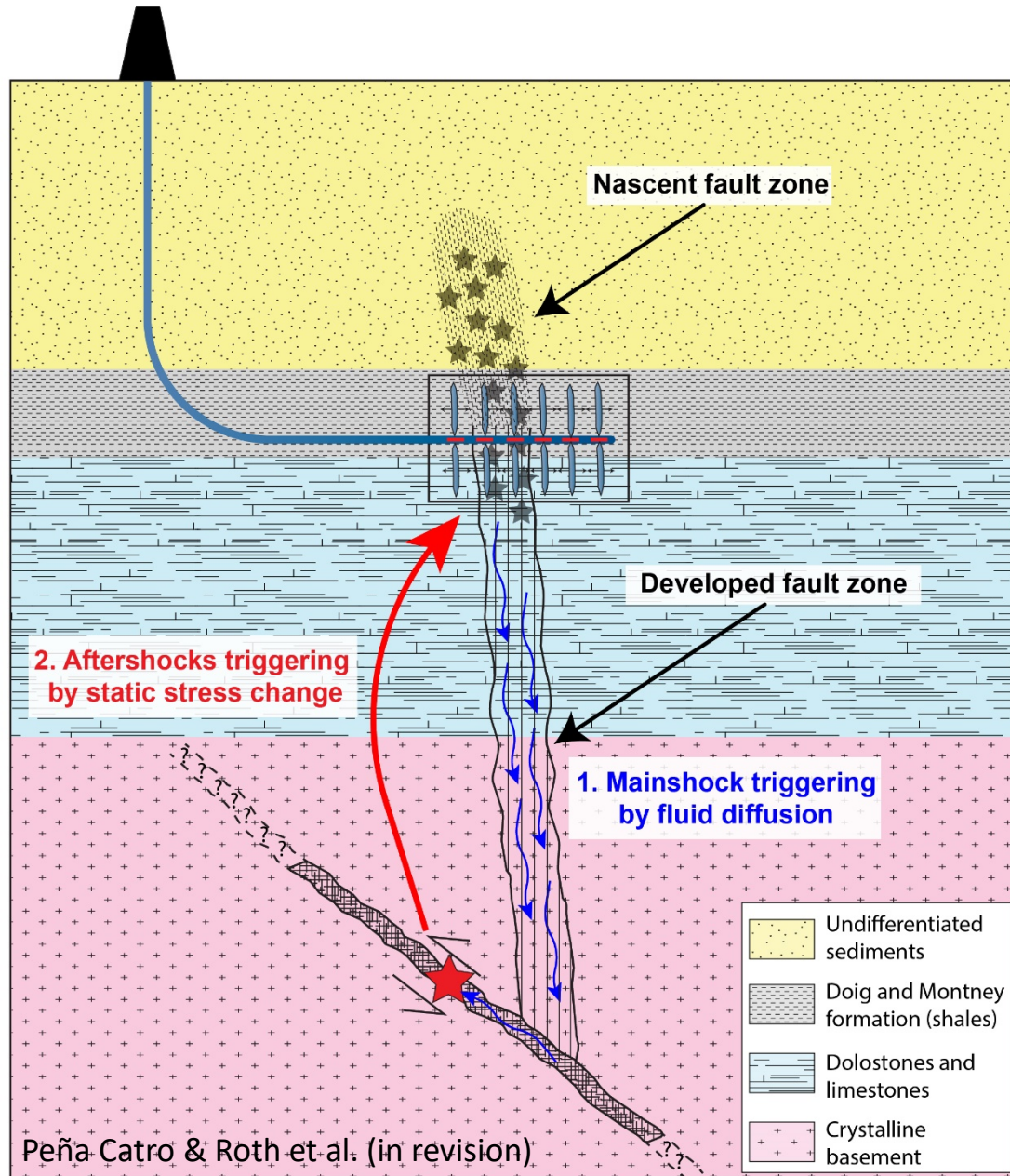


Δ CFS due to the coseismic slip of the $M_L 4.5$ mainshock, assuming a circular slip area under a static stress drop of 5.3 MPa shown in map view at 2 km depth, and cross-sections. Receiver fault kinematics (strike 245°, dip 88°, rake 0.4°) follow the focal mechanism solution of the largest ($M_L 4.2$) aftershock.

Peña Catro & Roth et al. (in revision)



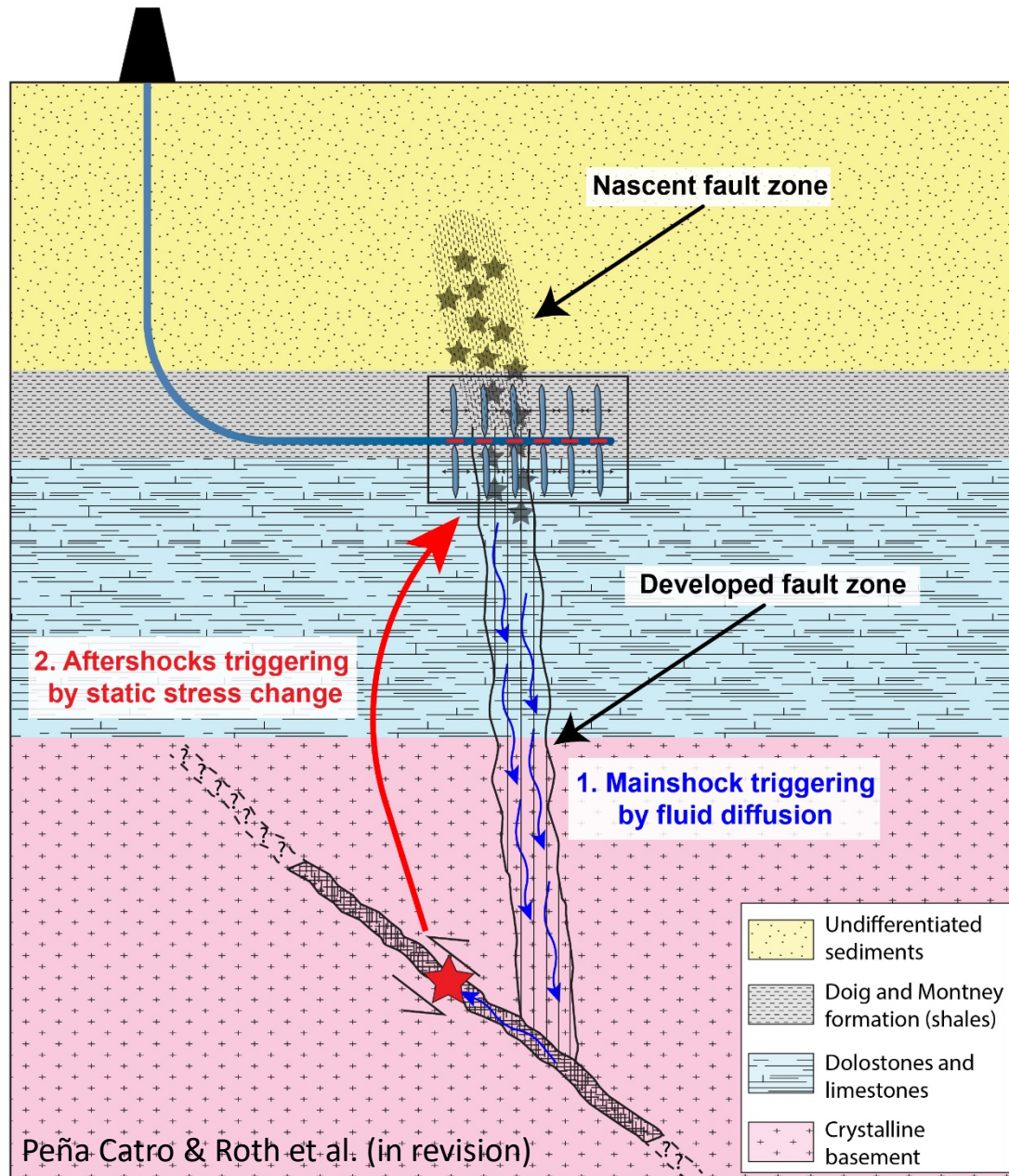
Conceptual model and conclusions



Two-step stress transfer during and shortly after HF stages:

- 1. Injected fluid migrates** (blue arrows) vertically through a **developed, permeable fracture network** to the basement fault and **pore pressure increase triggers the mainshock** (red star) fault plane.
- 2. Static Coulomb stress changes** due to the mainshock coseismic slip subsequently **trigger aftershocks** along a nascent fracture zone in the sedimentary layers

Conceptual model and conclusions



For both mainshock modeling scenarios, we hypothesize the **presence of a high-permeability conduit** connecting the Montney formation, where HF operations are occurring, with the crystalline basement, **facilitating fluid diffusion and the mainshocks triggering**

The November/December 2018 earthquake sequence is the result of a **combination of fluid-earthquake and earthquake-earthquake interactions** along a vertical strike-slip fault and a N-dipping thrust fault.